



Impact of nonextensivity on the transport coefficients of a magnetized hot and dense QCD matter

Shubhalaxmi Rath^a, Sadhana Dash^b

Department of Physics, Indian Institute of Technology Bombay, Mumbai 400076, India

Received: 17 March 2023 / Accepted: 17 September 2023 / Published online: 26 September 2023
© The Author(s) 2023

Abstract We have studied the impact of the nonextensivity on the transport coefficients related to charge and heat in thermal QCD. For this purpose, the electrical (σ_{el}), Hall (σ_H), thermal (κ) and Hall-type thermal (κ_H) conductivities are determined using the kinetic theory approach in association with the nonextensive Tsallis statistical mechanism. The effect of nonextensivity is encoded in the nonextensive Tsallis distribution function, where the deviation of the parameter q from 1 signifies the degree of nonextensivity in the concerned system. The thermal and electrical conductivities are found to increase with the introduction of nonextensivity, which means that the deviation of the medium from thermal equilibrium enhances both charge and heat transports. With the magnetic field, the deviations of σ_{el} , σ_H , κ and κ_H from their respective equilibrated values increase, whereas these deviations decrease with the chemical potential. We have also studied how the extent of the nonextensivity modulates the longevity of magnetic field. Present work is further extended to the study of some observables associated with the aforesaid transport phenomena, such as the Knudsen number and the elliptic flow within the nonextensive Tsallis framework.

1 Introduction

The collisions of ultrarelativistic heavy ions at Relativistic Heavy Ion Collider (RHIC) and Large Hadron Collider (LHC) provide strong evidences for the production of a deconfined state of quarks and gluons, known as quark-gluon plasma (QGP). This extreme state of matter can be achieved at high temperature and/or high density. In addition, for non-central events, strong magnetic fields are produced, whose strengths can vary between $eB = m_\pi^2$ ($\simeq 10^{18}$ Gauss) at RHIC and $eB = 15 m_\pi^2$ at LHC [1, 2]. These magnetic fields

become weak with time, where the energy scale associated with the temperature prevails over the energy scale related to the magnetic field. However, the electrically conducting medium ensures the longevity of such magnetic fields by the Lenz's law [3–5]. Some of the phenomena induced due to the presence of the magnetic field are the chiral magnetic effect [6, 7], the axial magnetic effect [8, 9], the nonlinear electromagnetic current [10, 11], the axial Hall current [12], the chiral vortical effect [13] etc. In recent years, the effects of magnetic field on QCD matter have been extensively studied, such as the thermodynamic and magnetic properties [14–17], the conductive properties [5, 18–24], the viscous properties [25–32], the photon and dilepton productions from QGP [33–36], the heavy quark diffusion [37], the magnetohydrodynamics [38, 39] etc. In these studies, the nonextensive approach has not been followed. In high energy physics community, the Tsallis nonextensive distribution has recently achieved great importance as it shows good fits of the transverse momentum distributions for a wide range of collision energies by STAR [40], PHENIX [41], ALICE [42] and CMS [43] collaborations. The nonextensive Tsallis statistics is considered as a generalization of the Boltzmann-Gibbs statistics, where the parameter q that measures the extent of non-equilibration is called the nonextensive Tsallis parameter. The theory groups have also started considering the nonextensive statistics in the study of thermodynamics, transport processes etc. [44–53]. In Langevin, Fokker-Planck, and/or Boltzmann type equations, this deviation can be incorporated through a nonextensive parameter or Tsallis parameter, q , where $q = 1$ represents the Boltzmann limit [54–57]. The relation between the parameter q and temperature fluctuations has been studied in Ref. [58], which observed that the deviation of q from unity measures the fluctuation in the temperature and there is no temperature fluctuation in the Boltzmann limit ($q = 1$).

The fits to the RHIC and LHC spectra suggest that q for the hadronic matter can deviate up to 1.08–1.2 [59–61] and

^a e-mail: shubhalaxmi@iitb.ac.in (corresponding author)

^b e-mail: sadhana@phy.iitb.ac.in

for a quark matter, the value of q deviates up to 1.22 [62]. The value of q should thus be considered as never being far from 1. Similar result for the parameter q has also been obtained in an analysis of the composition of final-state particles [58]. For large p_T results of particle production with $q > 1$, the freeze-out temperature becomes smaller in order to keep the particle yields the same, whereas, to compensate the decrease in the particle number, the baryon chemical potential increases with $q > 1$ [58]. Some observation shows that the Tsallis distribution leads to a much better chemical equilibrium than the Boltzmann distribution with $q = 1$ [58]. The nonextensivity can be inserted in the underlying dynamical model through the Tsallis nonextensive statistics. It is very beneficial to use the nonextensive Tsallis distribution function in the dynamical model itself to describe the characteristics of the medium in both the QGP and the freeze-out phases in order to study the effects on the bulk observables. The observables in heavy ion collisions, such as the transverse momentum spectra, the multiplicity fluctuations, the nuclear modification factor etc. are influenced by the nonextensive parameter q [63–65]. Thus, when the value of the nonextensive parameter gets deviated from unity, it is highly expected to leave some noticeable impacts on the properties of the matter produced in heavy ion collisions. Our present work attempts to see the possible deviation of the charge and heat transport properties of the QCD medium when q is slightly above unity.

In this paper, the transport coefficients related to charge conduction and heat conduction are calculated for the first time using a nonextensive relativistic Boltzmann transport equation in the relaxation time approximation, where the nonextensive Tsallis formalism has been incorporated. In addition, the thermal masses of particles and the weak magnetic field limit ($T^2 \gg |q_f B|$, where $|q_f|$ is the absolute electronic charge of the quark with flavor f) are considered in the calculations. This study is relevant to understand the effect of the nonextensivity on the transport coefficients in hot QCD matter. The effect on the lifetime of magnetic field is also studied by varying the value of parameter q up to 1.2. The aforesaid transport coefficients are important to understand the local equilibrium property, elliptic flow, hydrodynamic evolution of the strongly interacting matter etc. Thus, the deviation if any, of these transport coefficients due to the nonextensivity could also leave significant imprints on the observables used at heavy ion collisions.

The present paper is organized as follows. Section 2 is dedicated to the study of different charge and heat conductivities of a weakly magnetized QCD medium assuming a nonextensive scenario within the kinetic theory approach and its effect on the lifetime of magnetic field. The results on different conductivities are discussed in Sect. 3. In Sect. 4, some observables related to the aforesaid transport phenomena are studied. Section 5 presents the conclusions of this work.

2 Charge and heat conductivities in the nonextensive Tsallis framework

This section is devoted to the calculation of different charge and heat conductivities by using the relativistic Boltzmann transport equation in the relaxation time approximation, where the effect of nonextensivity is incorporated through the Tsallis distribution function. In particular, Sect. 2.1 contains the calculation of the conductivities at zero magnetic field, Sect. 2.2 shows the effect of nonextensivity on the lifetime of magnetic field and in Sect. 2.3, the conductivities are determined in a weak magnetic field.

2.1 Hot and dense QCD matter in the absence of magnetic field

In this subsection, we study the response of the nonextensivity to the charge and heat flow by calculating the electrical and thermal conductivities in the nonextensive Tsallis framework in the absence of magnetic field.

2.1.1 Response of the nonextensivity to the charge flow in a QCD medium

In the nonextensive Tsallis framework, the fermion distribution function is represented [66–68] as

$$f_q = \frac{1}{[1 + (q - 1)\beta\omega]^{\frac{1}{q-1}} + 1}, \quad \text{with } \beta\omega > 0, \quad (1)$$

where $\omega = \omega_f - \mu_f$ for quarks and $\bar{\omega} = \omega_f + \mu_f$ for anti-quarks, and q represents the nonextensive parameter. Here, $\omega_f = \sqrt{\mathbf{p}^2 + m_f^2}$ and μ_f is the chemical potential of quark with flavor f . The deviation of q from unity signifies the nonextensivity of the system. At high temperatures, Fermi–Dirac statistics (for fermions) and Bose–Einstein statistics (for bosons) behave like Boltzmann statistics, so, the above distribution function can be approximated to

$$f_q \approx [1 + (q - 1)\beta\omega]^{\frac{1}{1-q}}, \quad (2)$$

which is also the exponential factor in the usual Fermi–Dirac distribution function. Expansion of Eq. (2) around $q = 1$ gives

$$f_q = e^{-\beta\omega} + \frac{1}{2}(q - 1)\beta^2\omega^2 e^{-\beta\omega} + \frac{1}{24}(q - 1)^2(3\beta\omega - 8)\beta^3\omega^3 e^{-\beta\omega} + \dots, \quad (3)$$

where the first term in the right hand side represents the Boltzmann distribution function. One can see that at $q = 1$, only leading term remains, *i.e.* $f_q = e^{-\beta\omega}$. Thus, the limit $q \rightarrow 1$ yields the Boltzmann distribution and the deviation of q from unity explains how much the medium drives away

from the equilibrated thermal distribution of particles. Let us consider a nonextensive QCD medium having three flavors ($f = u, d, s$). When this medium comes under the effect of an external electric field, an electric current density is induced whose spatial component can be written as

$$J^i = \sum_f g_f \int \frac{d^3p}{(2\pi)^3 \omega_f} p^i [q_f \delta f_q + \bar{q}_f \delta \bar{f}_q], \tag{4}$$

where g_f, q_f (\bar{q}_f) and δf_q ($\delta \bar{f}_q$) are the degeneracy factor, electric charge and infinitesimal change in the nonextensive Tsallis distribution function for the quark (antiquark) of f th flavor, respectively. The Ohm's law states that the spatial current density is proportional to the electric field, with the proportionality factor being the electrical conductivity, *i.e.*,

$$J^i = \sigma_{el} E^i. \tag{5}$$

In order to determine the infinitesimal shift δf_q , we use the relativistic Boltzmann transport equation (RBTE) in the relaxation time approximation (RTA) within the nonextensive Tsallis mechanism, *i.e.*,

$$p^\mu \frac{\partial f'_q}{\partial x^\mu} + q_f F^{\rho\sigma} p_\sigma \frac{\partial f'_q}{\partial p^\rho} = -\frac{p_\nu u^\nu}{\tau_f} \delta f_q, \tag{6}$$

where $f'_q = \delta f_q + f_q$, $F^{\rho\sigma}$ denotes the electromagnetic field strength tensor whose components are associated with the electric and magnetic fields. In the above equation, the relaxation time for quarks (antiquarks), τ_f ($\tau_{\bar{f}}$) is given [69] by

$$\tau_{f(\bar{f})} = \frac{1}{5.1 T \alpha_s^2 \log(1/\alpha_s) [1 + 0.12(2N_f + 1)]}. \tag{7}$$

In the absence of magnetic field, in order to see the response of electric field, we use the components of $F^{\rho\sigma}$ related to only electric field. In addition, for a spatially homogeneous distribution function with the steady-state condition, one can use $\frac{\partial f'_q}{\partial \mathbf{r}} = 0$ and $\frac{\partial f'_q}{\partial t} = 0$. Thus, RBTE (6) takes the following form,

$$q_f \mathbf{E} \cdot \mathbf{p} \frac{\partial f'_q}{\partial p_0} + q_f p_0 \mathbf{E} \cdot \frac{\partial f'_q}{\partial \mathbf{p}} = -\frac{p_0}{\tau_f} \delta f_q. \tag{8}$$

Solving Eq. (8) with the nonextensive distribution function, we get δf_q as

$$\delta f_q = \frac{2\tau_f q_f \beta \mathbf{E} \cdot \mathbf{p}}{\omega_f} [1 + (q - 1)\beta(\omega_f - \mu_f)]^{\frac{q}{1-q}}. \tag{9}$$

Similarly, $\delta \bar{f}_q$ is calculated as

$$\delta \bar{f}_q = \frac{2\tau_{\bar{f}} \bar{q}_f \beta \mathbf{E} \cdot \mathbf{p}}{\omega_f} [1 + (q - 1)\beta(\omega_f + \mu_f)]^{\frac{q}{1-q}}. \tag{10}$$

Using the values of δf_q and $\delta \bar{f}_q$ in Eq. (4) and then comparing with Eq. (5), we get the electrical conductivity as

$$\sigma_{el} = \frac{\beta}{3\pi^2} \sum_f g_f q_f^2 \int dp \frac{p^4}{\omega_f^2} [\tau_f \{1 + (q - 1) \times \beta(\omega_f - \mu_f)\}^{\frac{q}{1-q}} + \tau_{\bar{f}} \{1 + (q - 1) \times \beta(\omega_f + \mu_f)\}^{\frac{q}{1-q}}]. \tag{11}$$

2.1.2 Response of the nonextensivity to the heat flow in a QCD medium

The flow of heat in a medium is regulated by the temperature and pressure gradients and the corresponding heat flow four-vector is defined as

$$Q_\mu = \Delta_{\mu\alpha} T^{\alpha\beta} u_\beta - h \Delta_{\mu\alpha} N^\alpha, \tag{12}$$

where the first and second terms in the right hand side are distinguished as the energy diffusion and the enthalpy diffusion, respectively. Here, $T^{\alpha\beta}$ is the energy-momentum tensor, N^α is the particle flow four-vector, the projection operator $\Delta_{\mu\alpha} = g_{\mu\alpha} - u_\mu u_\alpha$, the enthalpy per particle $h = (\varepsilon + P)/n$ with ε, P and n denoting the energy density, the pressure and the particle number density, respectively. N^α and $T^{\alpha\beta}$ are the first and second moments of the nonextensive distribution function, respectively.

$$N^\alpha = \sum_f g_f \int \frac{d^3p}{(2\pi)^3 \omega_f} p^\alpha [f_q + \bar{f}_q], \tag{13}$$

$$T^{\alpha\beta} = \sum_f g_f \int \frac{d^3p}{(2\pi)^3 \omega_f} p^\alpha p^\beta [f_q + \bar{f}_q]. \tag{14}$$

From N^α and $T^{\alpha\beta}$, one can get $n = N^\alpha u_\alpha, \varepsilon = u_\alpha T^{\alpha\beta} u_\beta$ and $P = -\Delta_{\alpha\beta} T^{\alpha\beta}/3$. In the rest frame of the heat bath, the heat flow is purely spatial, because it is orthogonal to the fluid four-velocity. Thus, the spatial component of heat flow is written as

$$Q^i = \sum_f g_f \int \frac{d^3p}{(2\pi)^3} \frac{p^i}{\omega_f} [(\omega_f - h_f) \delta f_q + (\omega_f - \bar{h}_f) \delta \bar{f}_q]. \tag{15}$$

Through the Navier–Stokes equation, the heat flow is associated with the gradients of temperature and pressure as

$$Q^i = -\kappa \delta^{ij} \left[\partial_j T - \frac{T}{\varepsilon + P} \partial_j P \right], \tag{16}$$

where κ represents the thermal conductivity. For the calculation of thermal conductivity, the electromagnetic field strength part can be dropped from the relativistic Boltzmann transport equation (6) and then expanding the gradient of the nonextensive distribution function in terms of the gradients

of flow velocity and temperature, we have

$$-p^\mu [1 + (q-1)\beta\omega]^{1-q} [(u_\alpha p^\alpha) \partial_\mu \beta + \beta \partial_\mu (u_\alpha p^\alpha) - \partial_\mu (\beta \mu)] = -\frac{u_\nu p^\nu}{\tau_f} \delta f_q. \quad (17)$$

After solving Eq. (17), we get δf_q as

$$\delta f_q = -\beta \tau_f [1 + (q-1)\beta\omega]^{1-q} \times \left[\frac{(\omega_f - h_f)}{T} v^j \left(\partial_j T - \frac{T}{nh_f} \partial_j P \right) + p_0 \frac{DT}{T} - \frac{p^\mu p^\alpha}{p_0} \nabla_\mu u_\alpha + TD \left(\frac{\mu_f}{T} \right) \right]. \quad (18)$$

Similarly, $\delta \bar{f}_q$ is determined as

$$\delta \bar{f}_q = -\beta \tau_{\bar{f}} [1 + (q-1)\beta\bar{\omega}]^{1-q} \times \left[\frac{(\omega_f - \bar{h}_f)}{T} v^j \left(\partial_j T - \frac{T}{n\bar{h}_f} \partial_j P \right) + p_0 \frac{DT}{T} - \frac{p^\mu p^\alpha}{p_0} \nabla_\mu u_\alpha - TD \left(\frac{\mu_f}{T} \right) \right]. \quad (19)$$

Substituting δf_q and $\delta \bar{f}_q$ in Eq. (15) and comparing with Eq. (16), we get the thermal conductivity as

$$\kappa = \frac{\beta^2}{6\pi^2} \sum_f g_f \int dp \frac{p^4}{\omega_f^2} \left[\tau_f (\omega_f - h_f)^2 \{1 + (q-1) \times \beta(\omega_f - \mu_f)\}^{1-q} + \tau_{\bar{f}} (\omega_f - \bar{h}_f)^2 \{1 + (q-1) \times \beta(\omega_f + \mu_f)\}^{1-q} \right]. \quad (20)$$

2.2 Effect of the nonextensivity on the lifetime of magnetic field

This subsection is dedicated to see how the nonextensivity affects the lifetime of magnetic field produced in the initial stages of the noncentral ultrarelativistic heavy ion collisions. Although this magnetic field is transient, but finite electrical conductivity elongates its lifetime significantly. This was discerned previously for a thermal distribution, where the nonextensive Tsallis parameter, $q = 1$. Now, it is interesting to observe how the longevity of magnetic field gets influenced when the nonextensive Tsallis parameter becomes deviated from unity.

Let a charged particle moves along x -direction, then there will be a production of magnetic field transverse to the trajectory of particle, which can be expressed [3] as

$$e\mathbf{B}_{\text{medium}} = \frac{e^2 b \sigma_{\text{el}}}{8\pi(t-x)^2} e^{-\frac{b^2 \sigma_{\text{el}}}{4(t-x)}} \hat{\mathbf{z}}, \quad (21)$$

where b is the impact parameter. In Eq. (21), the electrical conductivity depends on the time through the cooling

law, $T^3 \propto t^{-1}$. By taking the initial time 0.2 fm and initial temperature at 390 MeV, Fig. 1 is plotted which shows the variations of magnetic field with time (left panel) for $x = 0$, $b = 4$ fm and with impact parameter (right panel) for $x = 0$, $t = 1$ fm in an electrically conducting medium at different q values.

It is well known that the magnetic field decays very fast in vacuum, whereas the electrically conducting thermal medium helps in delaying the decay of magnetic field, where the parameter q has always been set to unity. The left panel of Fig. 1 displays that the decay of magnetic field gets further slowed down as the value of q increases slightly above unity. Thus, the nonextensivity of the thermal medium extends the lifetime of a nearly stable magnetic field. So, it is pertinent to study how the nonextensivity modifies the properties of the hot QCD matter in the absence as well as in the presence of magnetic field. It is also observed that, at initial time, the effect of the nonextensivity on the magnetic field is meagre and the effect becomes more conspicuous with the increase of the time. The right panel of Fig. 1 shows the effect of the nonextensivity on the magnetic field with the increase of impact parameter. It shows peak at some specific combination of magnetic field and impact parameter, and the height of the peak increases with the increase of deviation of q from unity, which occurs at a lower impact parameter. Thus, with the increase of the nonextensivity, the peak value of magnetic field increases.

2.3 Hot and dense QCD matter in a weak magnetic field

In this subsection, we study the response of the nonextensivity to the charge and heat flow by calculating the electrical, Hall, thermal and Hall-type thermal conductivities in the nonextensive Tsallis framework in the presence of a weak magnetic field.

2.3.1 Response of the nonextensivity to the charge flow in a weakly magnetized QCD medium

At finite magnetic field, the spatial component of electric current density is written as

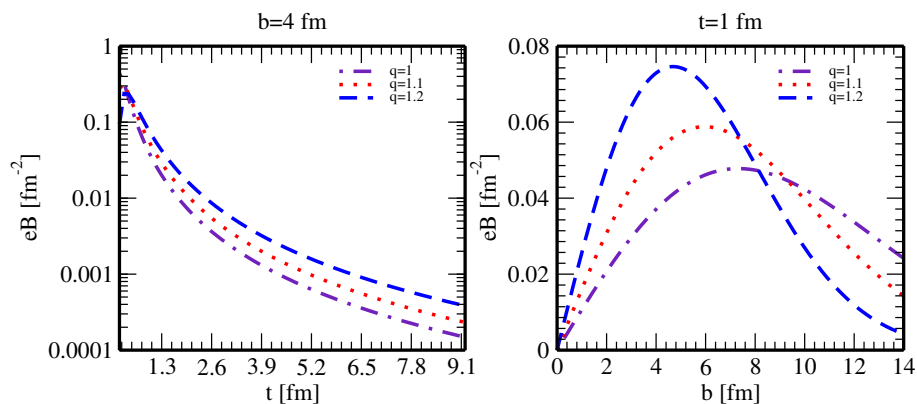
$$J^i = \sigma_0 \delta^{ij} E_j + \sigma_1 \epsilon^{ijk} b_k E_j + \sigma_2 b^i b^j E_j, \quad (22)$$

where σ_0 , σ_1 and σ_2 are various components of charge transport and $\mathbf{b} = \frac{\mathbf{B}}{B}$ is the direction of magnetic field. For $\mathbf{E} \perp \mathbf{B}$, the third term in the right hand side vanishes and thus, Eq. (22) becomes

$$J^i = \sigma^{ij} E_j = \left(\sigma_{\text{el}} \delta^{ij} + \sigma_{\text{H}} \epsilon^{ij} \right) E_j, \quad (23)$$

where ϵ^{ij} is the antisymmetric 2×2 unit matrix, $\sigma_0 = \sigma_{\text{el}}$ denotes the electrical conductivity and $\sigma_1 = \sigma_{\text{H}}$ represents the Hall conductivity. To determine the infinitesimal change

Fig. 1 Variation of magnetic field with time (left panel) and with impact parameter (right panel) at different values of the nonextensive parameter



in the nonextensive distribution function at finite magnetic field, let us rewrite RBTE (6) as

$$p^\mu \frac{\partial f'_q}{\partial x^\mu} + \mathcal{F}^\mu \frac{\partial f'_q}{\partial p^\mu} = -\frac{p_\nu u^\nu}{\tau_f} \delta f_q, \tag{24}$$

where $\mathcal{F}^\mu = q_f F^{\mu\nu} p_\nu = (p^0 \mathbf{v} \cdot \mathbf{F}, p^0 \mathbf{F})$ and the Lorentz force is defined as $\mathbf{F} = q_f (\mathbf{E} + \mathbf{v} \times \mathbf{B})$. For a spatially homogeneous distribution function with the steady-state condition, Eq. (24) gets simplified into

$$\mathbf{v} \cdot \mathbf{F} \frac{\partial f'_q}{\partial p_0} + \mathbf{F} \cdot \frac{\partial f'_q}{\partial \mathbf{p}} = -\frac{(f'_q - f_q)}{\tau_f}. \tag{25}$$

For $\mathbf{E} = E \hat{x}$ and $\mathbf{B} = B \hat{z}$, we have

$$\begin{aligned} \tau_f q_f E v_x \frac{\partial f'_q}{\partial p_0} + \tau_f q_f B v_y \frac{\partial f'_q}{\partial p_x} - \tau_f q_f B v_x \frac{\partial f'_q}{\partial p_y} \\ = f_q - f'_q - \tau_f q_f E \frac{\partial f_q}{\partial p_x}. \end{aligned} \tag{26}$$

To solve the above equation, we have followed an ansatz which is given [18] by

$$f'_q = f_q - \tau_f q_f \mathbf{E} \cdot \frac{\partial f_q}{\partial \mathbf{p}} - \mathbf{\Gamma} \cdot \frac{\partial f_q}{\partial \mathbf{p}}, \tag{27}$$

where the quantity $\mathbf{\Gamma}$ needs to be evaluated. Using ansatz (27) in Eq. (26) within the nonextensive framework, we get

$$\begin{aligned} \tau_f q_f E v_x \frac{\partial f'_q}{\partial p_0} + \beta [1 + (q-1)\beta\omega]^{\frac{q}{1-q}} \\ \times (\Gamma_x v_x + \Gamma_y v_y + \Gamma_z v_z) \\ - q_f B \tau_f \left(v_x \frac{\partial f'_q}{\partial p_y} - v_y \frac{\partial f'_q}{\partial p_x} \right) = 0. \end{aligned} \tag{28}$$

The partial derivatives in the above equation are determined as follows,

$$\begin{aligned} \frac{\partial f'_q}{\partial p_0} &= -\beta [1 + (q-1)\beta\omega]^{\frac{q}{1-q}} - q_f \tau_f \\ &\times E \frac{\beta v_x}{\omega_f} [1 + (q-1)\beta\omega]^{\frac{q}{1-q}} \\ &- q_f \tau_f E v_x \beta^2 q [1 + (q-1)\beta\omega]^{\frac{2q-1}{1-q}} \end{aligned}$$

$$\begin{aligned} -\frac{\beta}{\omega_f} [1 + (q-1)\beta\omega]^{\frac{q}{1-q}} (\Gamma_x v_x + \Gamma_y v_y + \Gamma_z v_z) \\ -\beta^2 q [1 + (q-1)\beta\omega]^{\frac{2q-1}{1-q}} (\Gamma_x v_x + \Gamma_y v_y + \Gamma_z v_z), \end{aligned} \tag{29}$$

$$\begin{aligned} \frac{\partial f'_q}{\partial p_x} &= -\beta v_x [1 + (q-1)\beta\omega]^{\frac{q}{1-q}} + q_f \tau_f \\ &\times E \frac{\beta}{\omega_f} [1 + (q-1)\beta\omega]^{\frac{q}{1-q}} \\ &- q_f \tau_f E \frac{\beta v_x^2}{\omega_f} [1 + (q-1)\beta\omega]^{\frac{q}{1-q}} - q_f \tau_f \\ &\times E \beta^2 v_x^2 q [1 + (q-1)\beta\omega]^{\frac{2q-1}{1-q}} \\ &+ \frac{\beta \Gamma_x}{\omega_f} [1 + (q-1)\beta\omega]^{\frac{q}{1-q}} \\ &- \frac{\beta v_x^2 \Gamma_x}{\omega_f} [1 + (q-1)\beta\omega]^{\frac{q}{1-q}} \\ &- \beta^2 v_x^2 q \Gamma_x [1 + (q-1)\beta\omega]^{\frac{2q-1}{1-q}} \\ &- \frac{\beta v_x^2 \Gamma_y}{\omega_f} [1 + (q-1)\beta\omega]^{\frac{q}{1-q}} \\ &- \beta^2 v_x v_y q \Gamma_y [1 + (q-1)\beta\omega]^{\frac{2q-1}{1-q}} \\ &- \frac{\beta v_x v_z \Gamma_z}{\omega_f} [1 + (q-1)\beta\omega]^{\frac{q}{1-q}} \\ &- \beta^2 v_x v_z q \Gamma_z [1 + (q-1)\beta\omega]^{\frac{2q-1}{1-q}}, \end{aligned} \tag{30}$$

$$\begin{aligned} \frac{\partial f'_q}{\partial p_y} &= -\beta v_y [1 + (q-1)\beta\omega]^{\frac{q}{1-q}} - q_f \tau_f \\ &\times E \frac{\beta v_x v_y}{\omega_f} [1 + (q-1)\beta\omega]^{\frac{q}{1-q}} \\ &- q_f \tau_f E \beta^2 v_x v_y q [1 + (q-1)\beta\omega]^{\frac{2q-1}{1-q}} \\ &- \frac{\beta v_x v_y \Gamma_x}{\omega_f} [1 + (q-1)\beta\omega]^{\frac{q}{1-q}} \\ &- \beta^2 v_x v_y q \Gamma_x [1 + (q-1)\beta\omega]^{\frac{2q-1}{1-q}} \\ &+ \frac{\beta \Gamma_y}{\omega_f} [1 + (q-1)\beta\omega]^{\frac{q}{1-q}} \end{aligned}$$

$$\begin{aligned}
& -\frac{\beta v_y^2 \Gamma_y}{\omega_f} [1 + (q-1)\beta\omega]^{1-q} \\
& -\beta^2 v_y^2 q \Gamma_y [1 + (q-1)\beta\omega]^{2q-1} \\
& -\frac{\beta v_y v_z \Gamma_z}{\omega_f} [1 + (q-1)\beta\omega]^{1-q} \\
& -\beta^2 v_y v_z q \Gamma_z [1 + (q-1)\beta\omega]^{2q-1}. \quad (31)
\end{aligned}$$

Now, substituting the expressions of the above partial derivatives in Eq. (28) and then simplifying by dropping the higher order velocity terms, we get

$$\begin{aligned}
& -q_f E \tau_f v_x + (\Gamma_x v_x + \Gamma_y v_y + \Gamma_z v_z) \\
& -\omega_c \tau_f (v_x \Gamma_y - v_y \Gamma_x) + \tau_f^2 \omega_c q_f E v_y = 0, \quad (32)
\end{aligned}$$

where $\omega_c = \frac{q_f B}{\omega_f}$ is known as cyclotron frequency. Equating the coefficients of v_x , v_y and v_z on both sides of Eq. (32) and then solving, we obtain

$$\Gamma_x = \frac{q_f E \tau_f (1 - \omega_c^2 \tau_f^2)}{1 + \omega_c^2 \tau_f^2}, \quad (33)$$

$$\Gamma_y = -\frac{2q_f E \omega_c \tau_f^2}{1 + \omega_c^2 \tau_f^2}, \quad (34)$$

$$\Gamma_z = 0. \quad (35)$$

Using the above values in the ansatz (27), δf_q is obtained as

$$\begin{aligned}
\delta f_q = & \left[2q_f E v_x \beta \left(\frac{\tau_f}{1 + \omega_c^2 \tau_f^2} \right) - 2q_f E v_y \beta \left(\frac{\omega_c \tau_f^2}{1 + \omega_c^2 \tau_f^2} \right) \right] \\
& \times [1 + (q-1)\beta(\omega_f - \mu_f)]^{1-q}. \quad (36)
\end{aligned}$$

Similarly, $\delta \bar{f}_q$ is found out to be

$$\begin{aligned}
\delta \bar{f}_q = & \left[2\bar{q}_f E v_x \beta \left(\frac{\tau_{\bar{f}}}{1 + \omega_c^2 \tau_{\bar{f}}^2} \right) - 2\bar{q}_f E v_y \beta \left(\frac{\omega_c \tau_{\bar{f}}^2}{1 + \omega_c^2 \tau_{\bar{f}}^2} \right) \right] \\
& \times [1 + (q-1)\beta(\omega_f + \mu_f)]^{1-q}. \quad (37)
\end{aligned}$$

Substituting the expressions of δf_q and $\delta \bar{f}_q$ in Eq. (4) and then comparing with Eq. (23), the electrical and Hall conductivities are calculated as

$$\begin{aligned}
\sigma_{\text{el}} = & \frac{\beta}{3\pi^2} \sum_f g_f q_f^2 \int d\mathbf{p} \frac{p^4}{\omega_f^2} \\
& \times \left[\frac{\tau_f}{1 + \omega_c^2 \tau_f^2} [1 + (q-1)\beta(\omega_f - \mu_f)]^{1-q} \right. \\
& \left. + \frac{\tau_{\bar{f}}}{1 + \omega_c^2 \tau_{\bar{f}}^2} [1 + (q-1)\beta(\omega_f + \mu_f)]^{1-q} \right], \quad (38)
\end{aligned}$$

$$\begin{aligned}
\sigma_{\text{H}} = & \frac{\beta}{3\pi^2} \sum_f g_f q_f^2 \int d\mathbf{p} \frac{p^4}{\omega_f^2} \left[\frac{\omega_c \tau_f^2}{1 + \omega_c^2 \tau_f^2} \right. \\
& \times [1 + (q-1)\beta(\omega_f - \mu_f)]^{1-q} \\
& \left. + \frac{\omega_c \tau_{\bar{f}}^2}{1 + \omega_c^2 \tau_{\bar{f}}^2} [1 + (q-1)\beta(\omega_f + \mu_f)]^{1-q} \right]. \quad (39)
\end{aligned}$$

2.3.2 Response of the nonextensivity to the heat flow in a weakly magnetized QCD medium

At finite magnetic field, the Navier–Stokes equation for heat flow takes the following form,

$$Q^i = - \left(\kappa_0 \delta^{ij} + \kappa_1 \epsilon^{ijk} b_k + \kappa_2 b^i b^j \right) \left[\partial_j T - \frac{T}{\varepsilon + P} \partial_j P \right], \quad (40)$$

where κ_0 , κ_1 and κ_2 represent different components of heat transport and $\mathbf{b} = \frac{\mathbf{B}}{B}$. If gradients of temperature and pressure are orthogonal to the magnetic field, then the third term in the right hand side vanishes and thus, Eq. (40) becomes

$$Q^i = - \left(\kappa \delta^{ij} + \kappa_{\text{H}} \epsilon^{ij} \right) \left[\partial_j T - \frac{T}{\varepsilon + P} \partial_j P \right]. \quad (41)$$

Here $\kappa_0 = \kappa$ represents the thermal conductivity and $\kappa_1 = \kappa_{\text{H}}$ denotes the Hall-type thermal conductivity. To determine these conductivities within the nonextensive Tsallis mechanism, we rewrite Eq. (24) using the ansatz (27) as

$$\begin{aligned}
& L + \beta [1 + (q-1)\beta\omega]^{1-q} (\Gamma_x v_x + \Gamma_y v_y + \Gamma_z v_z) \\
& - q_f B \tau_f \left(v_x \frac{\partial f'_q}{\partial p_y} - v_y \frac{\partial f'_q}{\partial p_x} \right) = 0, \quad (42)
\end{aligned}$$

where $L = \frac{\tau_f}{p_0} p^\mu \frac{\partial f_q}{\partial x^\mu}$. We note that, for the calculation of heat transport coefficients, we have dropped the electric field part from the relativistic Boltzmann transport equation. Since magnetic field is taken along z-direction and the gradients of temperature and pressure are orthogonal to the magnetic field, no explicit dependence of magnetic field on the temperature and pressure gradients along z-direction can be observed. Now, L is calculated as

$$\begin{aligned}
L = & \tau_f \beta^2 [1 + (q-1)\beta\omega]^{1-q} (\omega_f - h_f) \\
& \times v_x \left(\partial^x T - \frac{T}{nh_f} \partial^x P \right) \\
& + \tau_f \beta^2 [1 + (q-1)\beta\omega]^{1-q} \\
& \times (\omega_f - h_f) v_y \left(\partial^y T - \frac{T}{nh_f} \partial^y P \right) \\
& + \tau_f \beta [1 + (q-1)\beta\omega]^{1-q} \\
& \times \left[p_0 \frac{DT}{T} - \frac{p^\mu p^\alpha}{p_0} \nabla_\mu u_\alpha + TD \left(\frac{\mu_f}{T} \right) \right], \quad (43)
\end{aligned}$$

where $D = u^\mu \partial_\mu$ and $\nabla_\mu = \partial_\mu - u_\mu u_\nu \partial^\nu$. Substituting the values of L , $\frac{\partial f'_q}{\partial p_x}$ and $\frac{\partial f'_q}{\partial p_y}$ in Eq. (42), and then simplifying by dropping the higher order velocity terms, we have

$$\begin{aligned} &\beta (\omega_f - h_f) v_x \left(\partial^x T - \frac{T}{nh_f} \partial^x P \right) + \frac{\Gamma_x v_x}{\tau_f} - \omega_c \Gamma_y v_x \\ &+ \beta (\omega_f - h_f) v_y \left(\partial^y T - \frac{T}{nh_f} \partial^y P \right) + \frac{\Gamma_y v_y}{\tau_f} + \omega_c \Gamma_x v_y \\ &+ \frac{\Gamma_z v_z}{\tau_f} + p_0 \frac{DT}{T} - \frac{p^\mu p^\alpha}{p_0} \nabla_\mu u_\alpha + TD \left(\frac{\mu_f}{T} \right) = 0. \end{aligned} \tag{44}$$

Equating the coefficients of v_x , v_y and v_z on both sides of Eq. (44) and then solving, we get

$$\begin{aligned} \Gamma_x &= -\frac{\beta \tau_f (\omega_f - h_f)}{(1 + \omega_c^2 \tau_f^2)} \left(\partial^x T - \frac{T}{nh_f} \partial^x P \right) \\ &\quad - \frac{\beta \omega_c \tau_f^2 (\omega_f - h_f)}{(1 + \omega_c^2 \tau_f^2)} \left(\partial^y T - \frac{T}{nh_f} \partial^y P \right), \end{aligned} \tag{45}$$

$$\begin{aligned} \Gamma_y &= -\frac{\beta \tau_f (\omega_f - h_f)}{(1 + \omega_c^2 \tau_f^2)} \left(\partial^y T - \frac{T}{nh_f} \partial^y P \right) \\ &\quad + \frac{\beta \omega_c \tau_f^2 (\omega_f - h_f)}{(1 + \omega_c^2 \tau_f^2)} \left(\partial^x T - \frac{T}{nh_f} \partial^x P \right), \end{aligned} \tag{46}$$

$$\Gamma_z = 0. \tag{47}$$

Substituting the above values in ansatz (27), δf_q is calculated as

$$\begin{aligned} \delta f_q &= -\beta^2 [1 + (q - 1)\beta(\omega_f - \mu_f)]^{\frac{q}{1-q}} \\ &\quad \times \frac{\tau_f (\omega_f - h_f)}{(1 + \omega_c^2 \tau_f^2)} \left[v_x \left(\partial^x T - \frac{T}{nh_f} \partial^x P \right) \right. \\ &\quad \left. + v_y \left(\partial^y T - \frac{T}{nh_f} \partial^y P \right) \right] \\ &\quad - \beta^2 [1 + (q - 1)\beta(\omega_f - \mu_f)]^{\frac{q}{1-q}} \\ &\quad \times \frac{\omega_c \tau_f^2 (\omega_f - h_f)}{(1 + \omega_c^2 \tau_f^2)} \left[v_x \left(\partial^y T - \frac{T}{nh_f} \partial^y P \right) \right. \\ &\quad \left. - v_y \left(\partial^x T - \frac{T}{nh_f} \partial^x P \right) \right]. \end{aligned} \tag{48}$$

Similarly, $\delta \bar{f}_q$ is obtained as

$$\begin{aligned} \delta \bar{f}_q &= -\beta^2 [1 + (q - 1)\beta(\omega_f + \mu_f)]^{\frac{q}{1-q}} \\ &\quad \times \frac{\tau_{\bar{f}} (\omega_f - \bar{h}_f)}{(1 + \omega_c^2 \tau_{\bar{f}}^2)} \left[v_x \left(\partial^x T - \frac{T}{nh_f} \partial^x P \right) \right. \\ &\quad \left. + v_y \left(\partial^y T - \frac{T}{nh_f} \partial^y P \right) \right] \\ &\quad - \beta^2 [1 + (q - 1)\beta(\omega_f + \mu_f)]^{\frac{q}{1-q}} \end{aligned}$$

$$\begin{aligned} &\times \frac{\omega_c \tau_{\bar{f}}^2 (\omega_f - \bar{h}_f)}{(1 + \omega_c^2 \tau_{\bar{f}}^2)} \left[v_x \left(\partial^y T - \frac{T}{nh_f} \partial^y P \right) \right. \\ &\quad \left. - v_y \left(\partial^x T - \frac{T}{nh_f} \partial^x P \right) \right]. \end{aligned} \tag{49}$$

Using the values of δf_q and $\delta \bar{f}_q$ in Eq. (15) and then comparing with Eq. (41), the thermal and Hall-type thermal conductivities are determined as

$$\begin{aligned} \kappa &= \frac{\beta^2}{6\pi^2} \sum_f g_f \int dp \frac{p^4}{\omega_f^2} \left[\frac{\tau_f}{1 + \omega_c^2 \tau_f^2} (\omega_f - h_f)^2 \right. \\ &\quad \times [1 + (q - 1)\beta(\omega_f - \mu_f)]^{\frac{q}{1-q}} + \frac{\tau_{\bar{f}}}{1 + \omega_c^2 \tau_{\bar{f}}^2} \\ &\quad \left. \times (\omega_f - \bar{h}_f)^2 [1 + (q - 1)\beta(\omega_f + \mu_f)]^{\frac{q}{1-q}} \right], \end{aligned} \tag{50}$$

$$\begin{aligned} \kappa_H &= \frac{\beta^2}{6\pi^2} \sum_f g_f \int dp \frac{p^4}{\omega_f^2} \left[\frac{\omega_c \tau_f^2}{1 + \omega_c^2 \tau_f^2} (\omega_f - h_f)^2 \right. \\ &\quad \times [1 + (q - 1)\beta(\omega_f - \mu_f)]^{\frac{q}{1-q}} + \frac{\omega_c \tau_{\bar{f}}^2}{1 + \omega_c^2 \tau_{\bar{f}}^2} \\ &\quad \left. \times (\omega_f - \bar{h}_f)^2 [1 + (q - 1)\beta(\omega_f + \mu_f)]^{\frac{q}{1-q}} \right]. \end{aligned} \tag{51}$$

The above analysis on the charge and heat conductivities is studied by considering the quasiparticle or thermal masses of particles within the quasiparticle model. Partons acquire thermal masses due to their interactions with the surrounding thermal medium. In a hot and dense QCD medium, the quasiparticle mass (squared) of quark up to one-loop is given [70,71] by

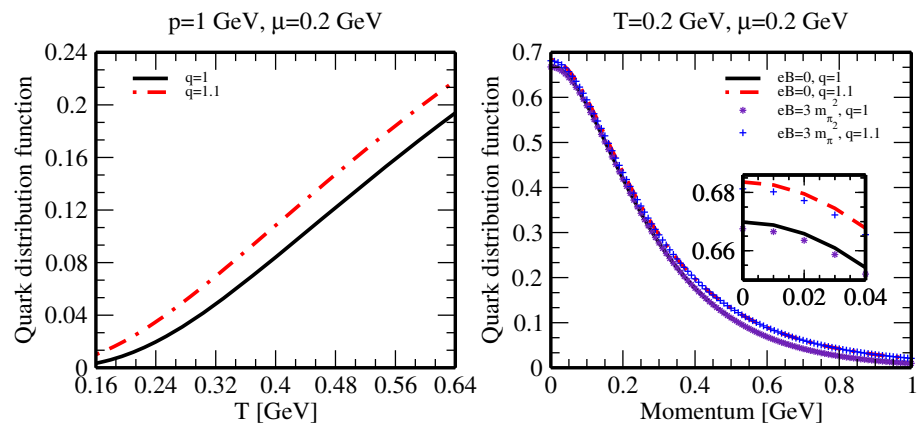
$$m_{fT}^2 = \frac{g^2 T^2}{6} \left(1 + \frac{\mu_f^2}{\pi^2 T^2} \right). \tag{52}$$

We note that, all flavors are assigned with the same chemical potential, *i.e.* $\mu_f = \mu$.

3 Results and discussions

In kinetic theory, the particle distribution functions embody most of the information on the transport coefficients and thus a study of the effect of nonextensivity on distribution function is first carried out before discussing its effect on the transport coefficients. Figure 2 shows the u quark distribution function in terms of temperature and momentum at a fixed chemical potential for different values of the nonextensive parameter and magnetic field. In particular, the left panel of Fig. 2 depicts the quark distribution function in terms of

Fig. 2 Variation of quark distribution function with temperature (left panel) and with momentum (right panel)



temperature at a fixed momentum and the right panel of Fig. 2 shows the same in terms of momentum at a fixed temperature. It is observed that the values are higher for the Tsallis distribution ($q = 1.1$) when compared with the Fermi–Dirac distribution ($q = 1$) over the shown range of temperature and the difference is not significant at low temperatures (left panel). On the other hand, the difference between the Tsallis distribution and the Fermi–Dirac distribution is exiguous at low momenta (right panel). Although the two types of distribution functions get slightly reduced in the presence of weak magnetic field as compared to zero magnetic field, the strength of Tsallis distribution function is always higher than that of the Fermi–Dirac distribution function.

We note that, in this work, the temperature and chemical potential are treated independent of q , *i.e.* $T \neq T(q)$ and $\mu \neq \mu(q)$. Thus, we plot the transport coefficients as functions of temperature at different q values, which gives the information on how the transport coefficients get affected by the nonextensivity when the temperature of the thermal medium changes. On the other hand, the thermal distribution functions of particles depend on all the aforesaid parameters, *i.e.* T , μ and q . How the distribution function depends on q is described above. Similarly, the energy-momentum tensor ($T^{\alpha\beta}$) and the particle flow four-vector (N^α) depend on q through the particle distribution function, thus the energy density ($\varepsilon = u_\alpha T^{\alpha\beta} u_\beta$) as well as the particle number density ($n = N^\alpha u_\alpha$) also depend on q parameter, in addition to their dependence on T and μ .

If one keeps the energy density or the particle number density at the same value in nonextensive Tsallis distribution ($q > 1$) and in Boltzmann type distribution ($q = 1$), then the Tsallis distribution, as compared to the Boltzmann one, leads to smaller values of T , *i.e.* with increasing q value, T decreases. For example, the references [50,58] had shown that, in order to keep the hadron yields (in high energy heavy ion collisions) the same in both nonextensive Tsallis and Boltzmann distributions, T is adjusted to lower values for increasing q value. Since the aim of the present paper is to see how the nonextensivity ($q > 1$) affects the transport coef-

ficients of the hot and dense QCD matter in kinetic theory approach for a range of temperature and chemical potential, we have not considered the correlation between q , T and μ .

3.1 Response functions of charge flow: electrical and Hall conductivities

Figure 3 depicts the variations of electrical (σ_{el}) and Hall (σ_H) conductivities of the hot QCD matter with temperature for different values of q . In particular, the upper panels of Fig. 3a, b show an enhancement in their magnitudes when q is slightly above unity and this increase is almost uniform over the entire range of temperature, thus it indicates that the nonextensivity facilitates the charge transport in hot QCD matter. The lower panels of Fig. 3a, b show the variations of the ratios of σ_{el} and σ_H at $q = 1.1$ and at $q = 1$ with T for different conditions of magnetic field and chemical potential. The nonextensive σ_{el} as well as σ_H get deviated from the corresponding thermally equilibrated values with the increase of magnetic field, whereas, the emergence of finite chemical potential brings σ_{el} and σ_H a bit closer to their equilibrated values. As compared to the Hall conductivity, the effect of the nonextensivity is more evident on the electrical conductivity in the weak magnetic field regime as σ_{el} is the dominant contribution and σ_H is a weak contribution of the charge transport in the said regime.

3.2 Response functions of heat flow: thermal and Hall-type thermal conductivities

The thermal (κ) and Hall-type thermal (κ_H) conductivities of the hot QCD matter are shown as functions of temperature for different values of q in Fig. 4. From the upper panels of Fig. 4a, b, one can see that both κ and κ_H increase with an increase of q . Thus, the nonextensivity amplifies the heat transport in hot QCD matter. Further, from the lower panels of Fig. 4a, b, it is observed that the presence of magnetic field increases the deviation of non-equilibrium κ and κ_H from their respective thermally equilibrated values, unlike the case

Fig. 3 Variations of **a** electrical conductivity and **b** Hall conductivity with temperature for different values of the nonextensive parameter at weak magnetic field and finite chemical potential

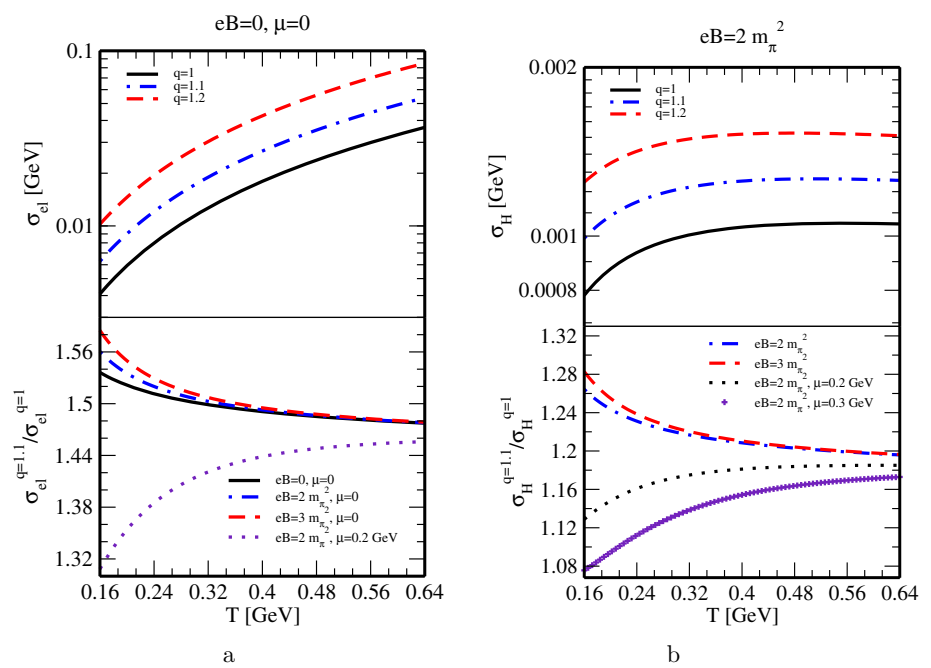
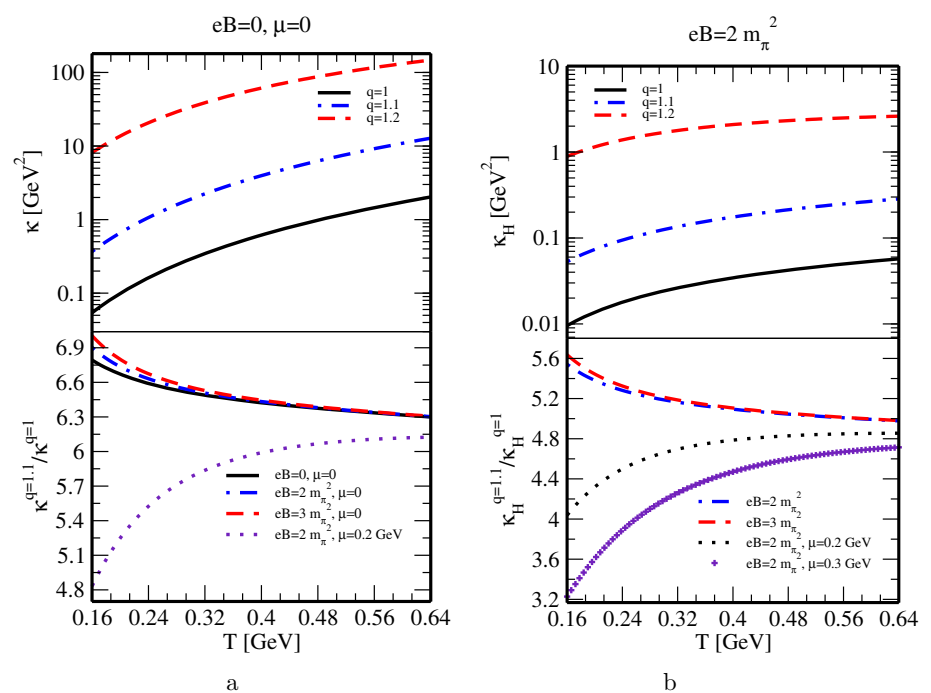


Fig. 4 Variations of **a** thermal conductivity and **b** Hall-type thermal conductivity with temperature for different values of the nonextensive parameter at weak magnetic field and finite chemical potential

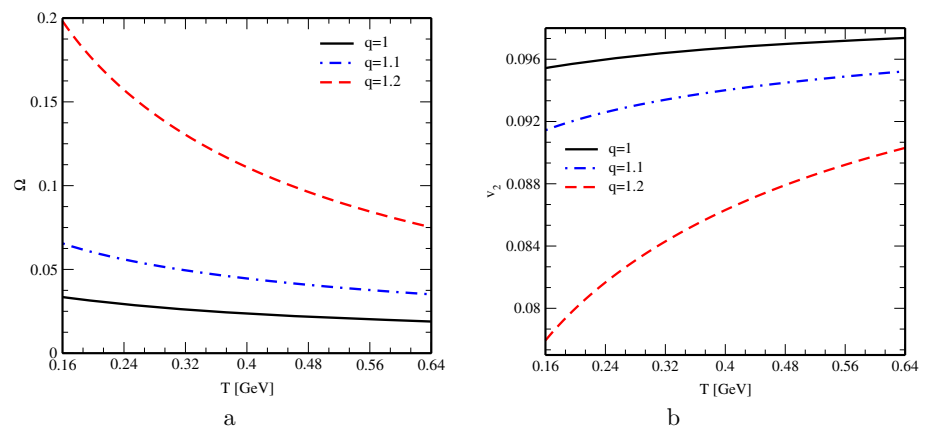


of finite chemical potential which decreases the deviation. Just like the charge transport case, the effect of nonextensivity is less pronounced for κ_H , because in the weak magnetic field regime, thermal conductivity is the dominant contribution of the heat transport. At high temperatures, the extra deviation occurred due to the magnetic field gets waned.

4 Observables

In this section, a detailed study on the Knudsen number and its association with elliptic flow coefficient is carried out. These quantities decipher the local equilibrium property of the medium and the extent of interactions among the produced particles in heavy ion collisions.

Fig. 5 Variations of **a** the Knudsen number and **b** the elliptic flow with temperature for different values of the nonextensive parameter



The Knudsen number is defined as the ratio of the mean free path (λ) to the characteristic length scale (l) of the medium, *i.e.* $\Omega = \lambda/l$. For an equilibrium system, l should be larger than λ . Since $\lambda = 3\kappa/(vC_V)$, the Knudsen number can be rewritten as

$$\Omega = \frac{3\kappa}{lvC_V}, \quad (53)$$

where v and C_V denote the relative speed and the specific heat at constant volume, respectively. The Knudsen number quantifies the degree of separation between the microscopic and macroscopic length scales of the system. For the applicability of equilibrium hydrodynamics, these two length scales require to be sufficiently separated, *i.e.* Ω must be very small or less than unity. In this analysis, we have used $v \simeq 1$ and $l = 4$ fm, and determined C_V from the energy-momentum tensor through the relation, $C_V = \partial(u_\mu T^{\mu\nu} u_\nu)/\partial T$.

The elliptic flow (v_2) reflects the anisotropy which originates from the overlapping region of nuclei and measures the extent of interactions/reinteractions between the particles produced in the noncentral heavy ion collisions. The initial asymmetry in the geometry of the matter distribution manifests the azimuthal anisotropy, which gets converted into the momentum anisotropy, thus contributing towards the emergence of elliptic flow [72]. The deviation from equilibrium can decrease the magnitude of this flow and if the collisions are frequent enough, then the system drives towards local equilibrium. Thus, the elliptic flow provides the information about the onset of thermalization in heavy ion collisions. The elliptic flow can be defined in terms of the Knudsen number [73–75] as

$$v_2 = \frac{v_2^h}{1 + \frac{\Omega}{\Omega_0}}, \quad (54)$$

where v_2^h denotes the elliptic flow in the hydrodynamic limit ($\Omega \rightarrow 0$ limit) and Ω_0 is the value of the Knudsen number obtained by observing the transition between the hydrodynamic regime and the free streaming particle regime. According to the transport calculation in Ref. [75], $\Omega_0 \approx 0.7$ and

$v_2^h \approx 0.1$. Experimentally observed values of v_2 at RHIC [76,77] are found to be larger than the theoretical estimates due to the strongly interacting nature of quark gluon plasma. As per the Cu-Cu PHOBOS collaboration [78], the reason for this large magnitude is mainly attributed to the fluctuations in the nucleon positions, which get transmitted into the fluctuations in the almond shape, thus stemming larger values of v_2 [79]. The presence of external fields could also influence the elliptic flow, *e.g.* an enhancement in the elliptic flow due to the presence of magnetic fields had been observed in references [19,80].

Figure 5a, b show how the nonextensivity affects the Knudsen number and the elliptic flow, respectively. With the increase of q , the Knudsen number is found to increase, whereas the elliptic flow gets decreased as compared to their counterparts at $q = 1$. The increasing behavior of Ω with q is corroborated by the increase of both κ (upper panel of Fig. 4a) and C_V (Fig. 7), with the increase of the former one being larger than that of the latter one. The opposite behaviors of Ω and v_2 can be elucidated from Eq. (54), which shows that both Ω and v_2 are almost inversely proportional to each other. The increase of Ω with q describes that the mean free path approaches towards the characteristic length scale of the medium, thus taking the system a bit away from the local equilibrium state. This agrees with the fact that the deviation of q from unity drives the system towards its nonequilibrium state. As q increases, there is a decrease of the number of collisions, which results into a smaller anisotropic flow, hence v_2 gets waned. The reduction of elliptic flow with the enhancement of the nonextensivity can also be realized from the enhancement of thermal conductivity (through its dependence on mean free path) in the similar environment (Fig. 4a).

Figure 6a, b respectively depict the effects of magnetic field and chemical potential on the Knudsen number and the elliptic flow for a thermal medium with finite nonextensivity. From the above discussion (see Figs. 4a, 5a, 5b and 7), it is evident that the Knudsen number gets enhanced and the elliptic flow becomes reduced as q changes from 1 to 1.1. Now from Fig. 6a, it can be seen that the presence of magnetic

Fig. 6 Variations of **a** the Knudsen number and **b** the elliptic flow with temperature for different values of the nonextensive parameter at finite magnetic field and chemical potential

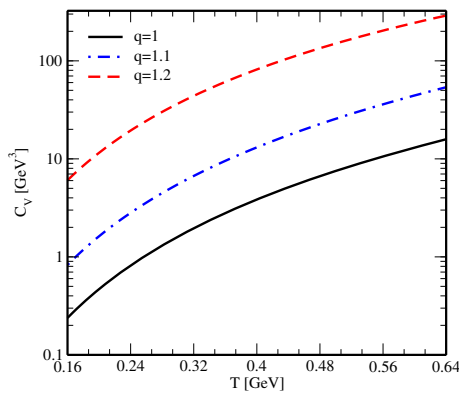
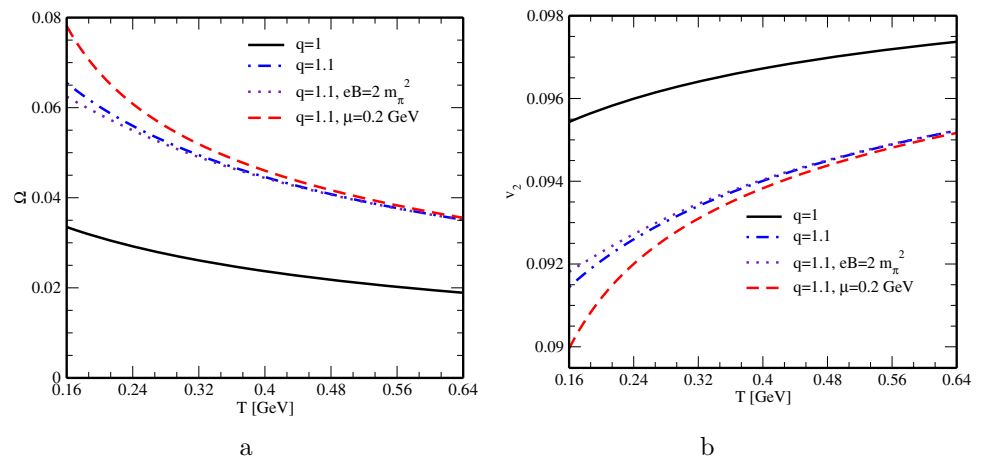


Fig. 7 Variation of the specific heat with temperature for different values of the nonextensive parameter

field pushes the Knudsen number towards its value at $q = 1$ (black solid line), contrary to the chemical potential which takes it further away from the said value. From Fig. 6b, it is inferred that the emergence of magnetic field shifts the elliptic flow towards its value at $q = 1$ (black solid line), whereas chemical potential further deviates it away from this value. The main reason behind the opposite effects of magnetic field and chemical potential on aforesaid observables is attributed to their opposite effects on the thermal conductivity (lower panel of Fig. 4a).

5 Conclusions

In this work, we focused on the effects of the nonextensivity on the conduction of charge and heat in hot and dense QCD matter at finite magnetic field. The electrical conductivity (σ_{el}) and the thermal conductivity (κ) were calculated using the relativistic Boltzmann transport equation in the kinetic theory approach within the nonextensive Tsallis formalism. The effect of the finite magnetic field was also studied. The presence of magnetic field additionally introduced two transport coefficients, namely, the Hall conductivity (σ_H) and the

Hall-type thermal conductivity (κ_H), which were also studied using the nonextensive framework. The lifetime of magnetic field was observed to increase with an increase of the nonextensive parameter. The transport coefficients (σ_{el} , σ_H , κ and κ_H) were observed to increase with the increase of the nonextensivity of the medium. This could have an observable effect on some observables associated with the aforesaid transport coefficients, such as the Knudsen number, the elliptic flow etc. Since these observables carry the information about the local equilibrium property of the matter, interactions between produced particles in heavy ion collisions etc., one can comprehend how the nonextensivity influences them.

Acknowledgements One of us (S. R.) would like to thank the Indian Institute of Technology Bombay for the Institute postdoctoral fellowship. Sadhana Dash acknowledges the SERB Power Fellowship, SPF/2022/000014 for the support on this work.

Data Availability Statement This manuscript has no associated data or the data will not be deposited. [Authors’ comment: All numerical data generated during this study are included in this published article.]

Open Access This article is licensed under a Creative Commons Attribution 4.0 International License, which permits use, sharing, adaptation, distribution and reproduction in any medium or format, as long as you give appropriate credit to the original author(s) and the source, provide a link to the Creative Commons licence, and indicate if changes were made. The images or other third party material in this article are included in the article’s Creative Commons licence, unless indicated otherwise in a credit line to the material. If material is not included in the article’s Creative Commons licence and your intended use is not permitted by statutory regulation or exceeds the permitted use, you will need to obtain permission directly from the copyright holder. To view a copy of this licence, visit <http://creativecommons.org/licenses/by/4.0/>.

Funded by SCOAP³. SCOAP³ supports the goals of the International Year of Basic Sciences for Sustainable Development.

References

1. V. Skokov, A. Illarionov, V. Toneev, *Int. J. Mod. Phys. A* **24**, 5925 (2009)
2. A. Bzdak, V. Skokov, *Phys. Lett. B* **710**, 171 (2012)

3. K. Tuchin, Adv. High Energy Phys. **2013**, 490495 (2013)
4. L. McLerran, V. Skokov, Nucl. Phys. A **929**, 184 (2014)
5. S. Rath, B.K. Patra, Phys. Rev. D **100**, 016009 (2019)
6. K. Fukushima, D.E. Kharzeev, H.J. Warringa, Phys. Rev. D **78**, 074033 (2008)
7. D.E. Kharzeev, L.D. McLerran, H.J. Warringa, Nucl. Phys. A **803**, 227 (2008)
8. V. Braguta, M.N. Chernodub, V.A. Goy, K. Landsteiner, A.V. Molochkov, M.I. Polikarpov, Phys. Rev. D **89**, 074510 (2014)
9. M.N. Chernodub, A. Cortijo, A.G. Grushin, K. Landsteiner, M.A.H. Vozmediano, Phys. Rev. B **89**, 081407 (R) (2014)
10. D.E. Kharzeev, Prog. Part. Nucl. Phys. **75**, 133 (2014)
11. D. Satow, Phys. Rev. D **90**, 034018 (2014)
12. S. Pu, S.Y. Wu, D.L. Yang, Phys. Rev. D **91**, 025011 (2015)
13. D.E. Kharzeev, D.T. Son, Phys. Rev. Lett. **106**, 062301 (2011)
14. S. Rath, B.K. Patra, J. High Energy Phys. **1712**, 098 (2017)
15. A. Bandyopadhyay, B. Karmakar, N. Haque, M.G. Mustafa, Phys. Rev. D **100**, 034031 (2019)
16. S. Rath, B.K. Patra, Eur. Phys. J. A **55**, 220 (2019)
17. B. Karmakar, R. Ghosh, A. Bandyopadhyay, N. Haque, M.G. Mustafa, Phys. Rev. D **99**, 094002 (2019)
18. B. Feng, Phys. Rev. D **96**, 036009 (2017)
19. S. Rath, S. Dash, Eur. Phys. J. A **59**, 25 (2023)
20. K. Hattori, D. Satow, Phys. Rev. D **94**, 114032 (2016)
21. L. Thakur, P.K. Srivastava, Phys. Rev. D **100**, 076016 (2019)
22. K. Fukushima, Y. Hidaka, Phys. Rev. Lett. **120**, 162301 (2018)
23. S. Rath, B.K. Patra, Eur. Phys. J. C **80**, 747 (2020)
24. M. Kurian, S. Mitra, S. Ghosh, V. Chandra, Eur. Phys. J. C **79**, 134 (2019)
25. G.S. Denicol et al., Phys. Rev. D **98**, 076009 (2018)
26. A. Das, H. Mishra, R.K. Mohapatra, Phys. Rev. D **100**, 114004 (2019)
27. Seung-I. Nam, Chung W. Kao, Phys. Rev. D **87**, 114003 (2013)
28. S. Rath, S. Dash, Eur. Phys. J. C **82**, 797 (2022)
29. S. Rath, B.K. Patra, Phys. Rev. D **102**, 036011 (2020)
30. S. Rath, B.K. Patra, Eur. Phys. J. C **81**, 139 (2021)
31. K. Hattori, X.-G. Huang, D.H. Rischke, D. Satow, Phys. Rev. D **96**, 094009 (2017)
32. S. Li, Ho. U. Yee, Phys. Rev. D **97**, 056024 (2018)
33. H. van Hees, C. Gale, R. Rapp, Phys. Rev. C **84**, 054906 (2011)
34. C. Shen, U.W. Heinz, J.-F. Paquet, C. Gale, Phys. Rev. C **89**, 044910 (2014)
35. K. Tuchin, Phys. Rev. C **88**, 024910 (2013)
36. K.A. Mamo, J. High Energy Phys. **1308**, 083 (2013)
37. K. Fukushima, K. Hattori, H.-U. Yee, Y. Yin, Phys. Rev. D **93**, 074028 (2016)
38. V. Roy, S. Pu, L. Rezzolla, D. Rischke, Phys. Lett. B **750**, 45 (2015)
39. G. Inghirami, L. Del Zanna, A. Beraudo, M.H. Moghaddam, F. Becattini, M. Bleicher, Eur. Phys. J. C **76**, 659 (2016)
40. B.I. Abelev et al. [STAR Collaboration], Phys. Rev. C **75**, 064901 (2007)
41. A. Adare et al. [PHENIX Collaboration], Phys. Rev. C **83**, 064903 (2011)
42. K. Aamodt et al. [ALICE Collaboration], Eur. Phys. J. C **71**, 1655 (2011)
43. V. Khachatryan et al. [CMS Collaboration], J. High Energy Phys. JHEP **1105**, 064 (2011)
44. C. Tsallis, J. Stat. Phys. **52**, 479 (1988)
45. C. Tsallis, *Introduction to Nonextensive Statistical Mechanics: Approaching a Complex World* (Springer, New York, 2009)
46. C. Tsallis, Eur. Phys. J. A **40**, 257 (2009)
47. C. Beck, Eur. Phys. J. A **40**, 267 (2009)
48. G. Kaniadakis, Eur. Phys. J. A **40**, 275 (2009)
49. T. Kodama, T. Koide, Eur. Phys. J. A **40**, 289 (2009)
50. G. Wilk, Z. Włodarczyk, Eur. Phys. J. A **40**, 299 (2009)
51. W.M. Alberico, A. Lavagno, Eur. Phys. J. A **40**, 313 (2009)
52. T.S. Biró, G. Purcsel, K. Ürmösy, Eur. Phys. J. A **40**, 325 (2009)
53. M. Alqahtani, N. Demir, M. Strickland, Eur. Phys. J. C **82**, 973 (2022)
54. D.B. Walton, J. Rafelski, Phys. Rev. Lett. **84**, 31 (2000)
55. G. Kaniadakis, Phys. Lett. A **288**, 283 (2001)
56. T.S. Biró, A. Jakovac, Phys. Rev. Lett. **94**, 132302 (2005)
57. T.J. Sherman, J. Rafelski, Lect. Notes Phys. **633**, 377 (2004)
58. J. Cleymans, G. Hamar, P. Levai, S. Wheaton, J. Phys. G Nucl. Part. Phys. **36**, 064018 (2009)
59. Z. Tang, Y. Xu, L. Ruan, G. van Buren, F. Wang, Z. Xu, Phys. Rev. C **79**, 051901 (2009)
60. M. Shao, L. Yi, Z. Tang, H. Chen, C. Li, Z. Xu, J. Phys. G Nucl. Part. Phys. **37**, 085104 (2010)
61. F. Siklér, EPJ Web Conf. **13**, 03002 (2011)
62. T.S. Biró, K. Ürmösy, J. Phys. G Nucl. Part. Phys. **36**, 064044 (2009)
63. C. Beck, E.G.D. Cohen, Phys. A **322**, 267 (2003)
64. T.S. Biró, K. Ürmösy, G.G. Barnaföldi, J. Phys. G Nucl. Part. Phys. **35**, 044012 (2008)
65. S. Tripathy, T. Bhattacharyya, P. Garg, P. Kumar, R. Sahoo, J. Cleymans, Eur. Phys. J. A **52**, 289 (2016)
66. J.M. Conroy, H.G. Miller, Phys. Rev. D **78**, 054010 (2008)
67. T.S. Biró, E. Molnár, Phys. Rev. C **85**, 024905 (2012)
68. J. Cleymans, D. Worku, J. Phys. G Nucl. Part. Phys. **39**, 025006 (2012)
69. A. Hosoya, K. Kajantie, Nucl. Phys. B **250**, 666 (1985)
70. E. Braaten, R.D. Pisarski, Phys. Rev. D **45**, R1827 (1992)
71. A. Peshier, B. Kämpfer, G. Soff, Phys. Rev. D **66**, 094003 (2002)
72. J.-Y. Ollitrault, Phys. Rev. D **46**, 229 (1992)
73. R.S. Bhalerao, J.-P. Blaizot, N. Borghini, J.-Y. Ollitrault, Phys. Lett. B **627**, 49 (2005)
74. H.-J. Drescher, A. Dumitru, C. Gombeaud, J.-Y. Ollitrault, Phys. Rev. C **76**, 024905 (2007)
75. C. Gombeaud, J.-Y. Ollitrault, Phys. Rev. C **77**, 054904 (2008)
76. H. Masui [PHENIX Collaboration], Nucl. Phys. A **774**, 511 (2006)
77. G. Wang [STAR Collaboration], Nucl. Phys. A **774**, 515 (2006)
78. S. Manly et al. [PHOBOS Collaboration], Nucl. Phys. A **774**, 523 (2006)
79. R.S. Bhalerao, J.Y. Ollitrault, Phys. Lett. B **641**, 260 (2006)
80. R.K. Mohapatra, P.S. Saumia, A.M. Srivastava, Mod. Phys. Lett. A **26**, 2477 (2011)